Interface engineering towards efficient and stable perovskite solar cell modules

Haifei Wang[1, 2, 7], Shuojian Su[1, 3, 4, 7], Yuetian Chen[1, 2, 5, 7], Meng Ren[1], Shaowei Wang[1], Yao Wang[3], Chen Zhu[3, 4], Yanfeng Miao[1, 2, 5], Chuying Ouyang[3, 4, 6]* and Yixin Zhao[1, 2, 3, 5]**

[1]School of Environmental Science and Engineering, Frontiers Science Center for Transformative Molecules, Shanghai Jiao Tong University, Shanghai 200240, China

[2]Shanghai Non-carbon Energy Conversion and Utilization Institute, Shanghai 200240, China

[3]Center of Future Photovoltaics Research, Global Institute of Future Technology, Shanghai Jiao Tong University (SJTU-GIFT), Shanghai 200240, China

[4]Fujian Science & Technology Innovation Laboratory for Energy Devices of China, Fujian 352100, China

[5]State Key Lab of Metal Matrix Composites, Shanghai Jiao Tong University, Shanghai 200240, China

[6]Department of Physics, Laboratory of Computational Materials Physics, Jiangxi Normal University, Nanchang 330022, China

[7]These authors contributed equally: Haifei Wang, Shuojian Su and Yuetian Chen

**Correspondence to: yanfengmiao@sjtu.edu.cn; cyouyang@jxnu.edu.cn; yixin.zhao@sjtu.edu.cn*

ABSTRACT

One major challenge hindering the scaling up of perovskite photovoltaics is the significant efficiency drop that occurs as the device area increases, primarily due to the inhomogeneous distribution of native impurities, including uncoordinated Pb^{2+}, PbI_2 and δ-$FAPbI_3$ non-perovskite, which could induce unfavored non-radiative recombination and inferior charge transport and extraction. Here we report a comprehensive impurity-healing interface engineering using a rationally designed multi-functional cation of 2-(1-cyclohexenyl)ethyl ammonium ($CHEA^+$). We found that $CHEA^+$ can effectively convert the native impurities in formamidinium lead iodide ($FAPbI_3$) perovskite film into stable 2D $CHEA_2PbI_4$ perovskite with high hole mobility. Besides, the formed 2D $CHEA_2PbI_4$ not only distribute on the surface of 3D perovskite but also vertically penetrate into the grain boundaries. Therefore $CHEA^+$ treatment could homogeneously heal the defects on large-area perovskite films and provide a high-speed channel for charge carrier transport, resulting in improved efficiency and enhanced stability of PSMs. As a result, small-area $FAPbI_3$-based PSCs can reach a champion PCE of 25.86% and large-area module with an aperture area of 715.1 cm^2 reached a certified efficiency of 22.46%, which is among the highest values for modules.

KEY WORDS

Perovskite Solar Cells; Perovskite solar Modules; Two-dimensional Perovskite; Defect Passivation.

1. INTRODUCTION

Small-area (~0.1 cm^2) perovskite solar cells (PSCs) have reached high power conversion efficiencies (PCEs) over 25%, comparable to crystalline silicon solar cells.[1] However, unlike mono-component crystalline silicon with covalent bond structure, when enlarging the cell area over 200 cm^2, there is always an obvious efficiency drop caused by a broad library of impurities including PbI_2, non-perovskite yellow phase, and trap states.[2] The fundamental reason for this phenomenon is that, during the crystallization process of multi-component perovskites at large scales, various types of impurities and compositional segregation occur inevitably. These issues tend to have a reduced effect on small-area devices and can be resolved or avoided through a variety of strategies. However, for large area perovskite solar modules (PSMs), these impurities not only severely restrict the performance, but also negatively affect the operational stability of PSMs.[3] Here, we develop an impurity-healing interface engineering strategy to well address this issue both in small-area PSCs and large-scale PSMs by the introduction of 2-(1-cyclohexenyl)ethyl ammonium iodide (CHEAI). The above-mentioned impurities on $FAPbI_3$ films can be converted into stable 2D $CHEA_2PbI_4$ that leads to a uniform defect passivation, and provides high-speed channels for efficient carrier extraction. As a result, a certified PCE of 22.46% was achieved on a submodule (aperture area of 715.1 cm^2), well demonstrating the scaling-up feasibility of this impurity-healing interface engineering route.

2. RESULTS AND DISCUSSION

2.1 Impurity-healing of perovskite films

Grazing incidence wide-angle X-ray scattering (GIWAXS) measurement in Fig. 1a shows that there are PbI_2 and δ-$FAPbI_3$ in the as-prepared $FAPbI_3$ film (denoted as control film). After

CHEAI treatment (denoted as target film), the signal of impurity components (PbI_2 and δ-$FAPbI_3$) disappeared and a new signal at $q \approx 3.7\ nm^{-1}$ appeared, indicating that the impurity components are converted into 2D perovskite (Fig. 1b). GIWAXS measurement (inset of Fig. 1b) focusing on the 2D region confirms that, besides the out-of-plane orientation, there is also in-plane orientation for 2D perovskite, which provides high-speed channels for efficient carrier extraction. Cross-sectional high-resolution scanning transmission electron microscopy (HR-STEM) in Fig. 1c shows that the 2D $CHEA_2PbI_4$ layer not only covers the surface of α-$FAPbI_3$ film but also penetrates the grain boundaries, which provide a comprehensive impurity-healing to the perovskite film. It is now a common thought that the surface and grain boundaries are usually where the impurity components exist[2]. The CHEAI post treatment can transform these species into 2D perovskite, thus achieving the comprehensive healing of perovskite films (Fig. 1c). More importantly, the vertically grown 2D perovskite at grain boundaries is beneficial for charge transport by providing effective hole extraction channels from perovskite to HTL[4].

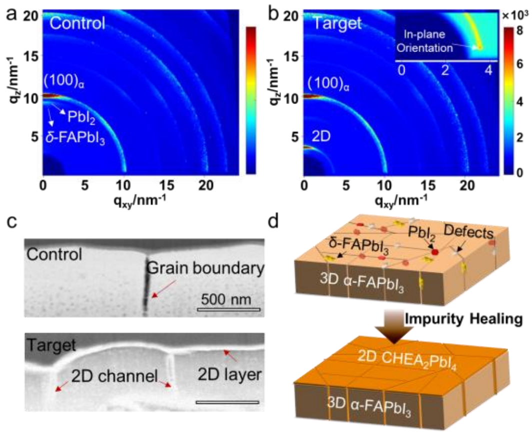

Fig. 1: (a) and (b) GIWAXS patterns. Inset in (b): zoomed-in GIWAXS pattern focusing on the in-plane orientation of 2D region. (c) Cross-sectional HR-STEM images of devices. (d) Schematic depiction of the CHEAI-induced impurity-healing process.

2.2 Characterizations of perovskite films

We treated part of control film with CHEAI/IPA and obtained the PL mapping image at the boundary (Fig. 2a). CHEAI-treated area has higher PL intensity and more homogeneous distribution than the control area. To explored the charge transport properties, we fabricated a "quasi-PSC" for conductive atomic force microscopy (c-AFM)

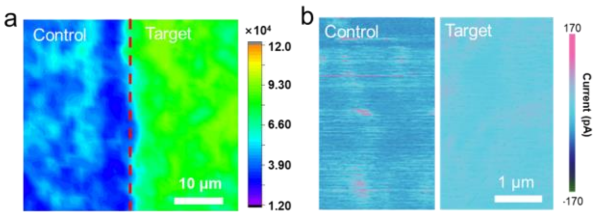

Fig. 2: (a) PL mapping result at the boundary between the control and target areas. (b) c-AFM images of control and target quasi-PSCs.

measurement with the structure of FTO/ETL/Perovskite/HTL and the c-AFM tip acting as the top electrode. The target quasi-PSC exhibits increased current and a more homogeneous current distribution (Fig. 2b), indicating efficient charge extraction, which is benefited from the construction of high-speed hole extraction channels and defect passivation.

2.3 Photovoltaic performance

As shown in Fig. 3a, CHEAI treated target devices can reach a high PCE of 25.86% with an FF over 86%. To further evaluate the impact of CHEAI on the photovoltaic performance of large area PSMs, we fabricated 30 × 30 cm^2 submodules with an aperture area of 715.1 cm^2. Fig. 3b presents the *J–V* curves of the champion PSM with a PCE of 22.80%, an FF of 82.68%. This excellent photovoltaic performance demonstrates the great potential of the impurity-healing interface engineering strategy in large scale fabrication of perovskite solar cells.

Fig. 2: (a) *J–V* curves of PSCs under reverse scan. (b)

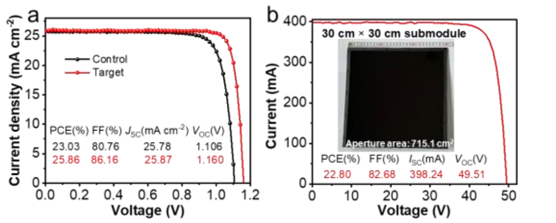

J–V curve of the champion target PSM and photograph (inset) of a 30 ×30 cm^2 PSM.

ACKNOWLEDGEMENTS

This work was supported by the National Natural Science Foundation of China (NSFC, Grant No. 22025505, 22220102002, 52203334 and 22209111), Natural Science Foundation of Shanghai (Grant No. 23ZR1432300 and 23ZR1428000), Shanghai Pujiang Program (Grant No. 22PJ1404700) and the Oceanic Interdisciplinary Program of Shanghai Jiao Tong University (Grant No. SL2022ZD105).

REFERENCES

[1] P. Chen, Y. Xiao, J. Hu, S. Li, D. Luo, R. Su, P. Caprioglio, P. Kaienburg, X. Jia, N. Chen, J. Wu, Y. Sui, P. Tang, H. Yan, T. Huang, M. Yu, Q. Li, L. Zhao, C.-H. Hou, Y.-W. You, J.-J. Shyue, D. Wang, X. Li, Q. Zhao, Q. Gong, Z.-H. Lu, H. J. Snaith, R. Zhu, *Nature* **2024**, *625*, 516.

[2] J. Park, J. Kim, H. S. Yun, M. J. Paik, E. Noh, H. J. Mun, M. G. Kim, T. J. Shin, S. I. Seok, *Nature* **2023**, *616*, 724.

[3] S. Macpherson, T. A. S. Doherty, A. J. Winchester, S. Kosar, D. N. Johnstone, Y. H. Chiang, K. Galkowski, M. Anaya, K. Frohna, A. N. Iqbal, S. Nagane, B. Roose, Z. Andaji-Garmaroudi, K. W. P. Orr, J. E. Parker, P. A. Midgley, K. M. Dani, S. D. Stranks, *Nature* **2022**, *607*, 294.

[4] H. Zhang, L. Pfeifer, S. M. Zakeeruddin, J. Chu, M. Gratzel, *Nat. Rev. Chem.* **2023**, *7*, 632.